AGU PUBLICATIONS

Geophysical Research Letters

RESEARCH LETTER

10.1002/2014GL059983

Key Points:
- Surface waves in the Arctic Ocean increase during periods of sea ice retreat
- Surface waves in the Arctic Ocean follow a nondimensional scaling law
- Surface waves in the Arctic Ocean are now evolving from seas into swells

Correspondence to:
J. Thomson,
jthomson@apl.uw.edu

Citation:
Thomson, J., and W. E. Rogers (2014), Swell and sea in the emerging Arctic Ocean, *Geophys. Res. Lett.*, *41*, 3136–3140, doi:10.1002/2014GL059983.

Received 21 MAR 2014
Accepted 17 APR 2014
Accepted article online 23 APR 2014
Published online 5 MAY 2014

Swell and sea in the emerging Arctic Ocean

Jim Thomson[1] and W. Erick Rogers[2]

[1]Applied Physics Laboratory, University of Washington, Seattle, Washington, USA, [2]Naval Research Laboratory, Stennis Space Center, Mississippi, USA

Abstract Ocean surface waves (sea and swell) are generated by winds blowing over a distance (fetch) for a duration of time. In the Arctic Ocean, fetch varies seasonally from essentially zero in winter to hundreds of kilometers in recent summers. Using in situ observations of waves in the central Beaufort Sea, combined with a numerical wave model and satellite sea ice observations, we show that wave energy scales with fetch throughout the seasonal ice cycle. Furthermore, we show that the increased open water of 2012 allowed waves to develop beyond pure wind seas and evolve into swells. The swells remain tied to the available fetch, however, because fetch is a proxy for the basin size in which the wave evolution occurs. Thus, both sea and swell depend on the open water fetch in the Arctic, because the swell is regionally driven. This suggests that further reductions in seasonal ice cover in the future will result in larger waves, which in turn provide a mechanism to break up sea ice and accelerate ice retreat.

1. Introduction

In the open ocean, surface waves (sea and swell) are a central feature of the air-water-ice interface, where significant exchanges of momentum, heat, and gases occur [*Steele et al.*, 1989; *Melville*, 1996]. At the coasts, surface waves can force circulation and cause erosion [*Battjes*, 1988]. Surface waves also can be a hazard to navigation and operations at sea. In the emerging Arctic Ocean, all of these wave processes are becoming significant to the natural and human systems [*Stephenson et al.*, 2011; *Showstack*, 2013]. The interaction of waves and ice is particularly complex, because ice can suppress waves by scattering and dissipating wave energy [*Squire et al.*, 1995; *Squire*, 2007], while the waves simultaneously break up the ice [*Dozaki et al.*, 1999; *Marko*, 2003]. Ice also has an indirect effect on surface waves, by setting the fetch available for wave generation and the distance available for wave evolution. This is the effect we study in this paper.

In the absence of ice, the dependence of ocean surface waves on fetch is a well-studied problem, and fetch has been found to be the limiting variable for wave generation in coastal regions and marginal seas [*Hasselmann et al.*, 1973]. Several empirical fits describe the evolution of waves along a fetch x acted on by a uniform wind U using the nondimensional scaling parameters of wave energy and fetch [*Young*, 1999]:

$$\mathcal{E} = \frac{g^2 H^2}{16 U^4}, \quad \mathcal{X} = \frac{gx}{U^2} \tag{1}$$

where H is significant wave height and g is gravity. Storm duration can be similarly scaled as $\mathcal{T} = \frac{gt}{U}$, and duration is often the limiting variable for wave growth in the open ocean [*Young*, 1999]. In practice, uniform winds are rarely observed, yet these existing empirical fetch laws often remain in agreement with observations [*Schwendeman et al.*, 2014]. For a pure wind sea (i.e., short waves forced by local winds), the Pierson–Moskowitz limit asserts a maximum nondimensional energy $\mathcal{E} = 3.64 \times 10^{-3}$ that occurs for a saturated sea state [*Pierson and Moskowitz*, 1964]. This limit remains debated and undervalidated, in part because most natural wave conditions include both sea and swell (i.e., long waves resulting from nonlocal winds) [*Alves et al.*, 2003]. Swell waves accumulate the energy in the wind sea and, given enough space and time, often exceed this limit.

Here we intentionally include conditions with both sea and swell and examine the large-scale effects of variable open water distances in the Arctic Ocean. This is in contrast to the strict definition of a fetch dependence, in which a pure wind sea achieves a local equilibrium between generation by wind forcing and dissipation by wave breaking [*Fontaine*, 2012]. Rather, we use the distance scale $\mathcal{X}$ to describe the overall space available for waves to be generated as a wind sea and then evolve to become swell.

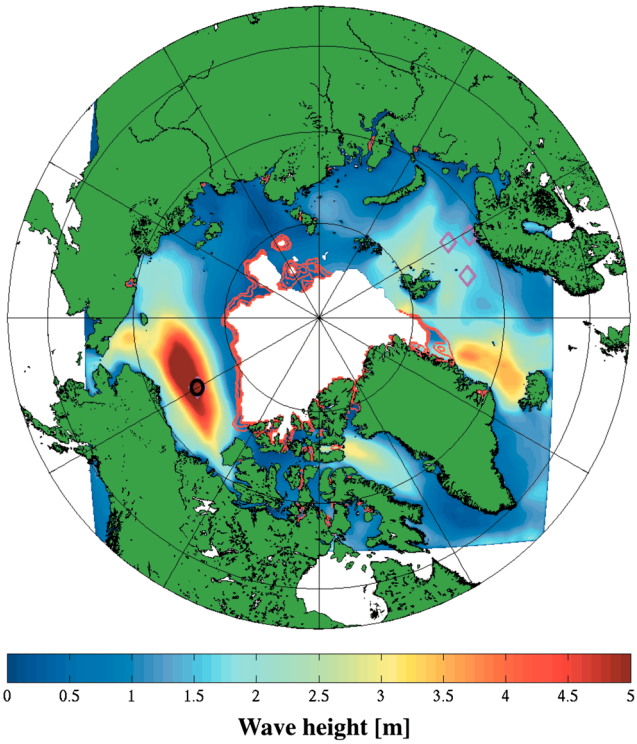

Figure 1. Example wave model hindcast during September 2012 storm. The map is centered on the North Pole, and the mooring location is indicated by the black circle north of Alaska. The color scale indicates significant wave height from 0 to 5 m.

In the modern Beaufort Sea, the open water distances change dramatically throughout the summer season, from essentially zero in April (sea ice cover maximum) to well over 1000 km in September (sea ice cover minimum). In recent years, the seasonal ice retreat has expanded dramatically [*Stroeve et al.*, 2005, 2008; *Simmonds and Keay*, 2009], leaving much of the Beaufort Sea ice free at the end of summer. For example, on 18 September 2012 strong winds (up to 18 m s^{-1}) generated 5 m wave heights in the ice-free central Beaufort Sea (Figure 1). These conditions were measured in situ using a mooring near the middle of the basin and modeled using a spectral wave action balance code (WAVEWATCH III ®). There are few previous studies of waves in the Arctic Ocean; they have focused mostly near the coasts or on local effects [*Francis et al.*, 2011; *Squire et al.*, 2009; *Bogucki et al.*, 2013]. Of the previous studies, *Francis et al.* [2011] in particular showed a strong trend of increasing surface wave heights in the Arctic. The observations reported here are the only known wave measurements in the central Beaufort Sea, because until recently the region remained ice covered throughout the summer and there were no waves to measure.

2. Methods

Wave observations were collected using a 600 kHz Nortek Acoustic Wave and Current (AWAC) sensor deployed on a subsurface mooring at 75°N, 150°W as part of the Beaufort Gyre Exploration Project. The AWAC was mounted at the top (50 m below the surface) of the 3000 m mooring, looking up to the surface. The AWAC uses sonar pings to determine the distance from the instrument to the sea surface, and this distance is recorded at 1 Hz for 1024 s at the beginning of each hour. These records are processed using a fast Fourier transform to determine the wave energy spectra, as well as the significant wave height (defined as 4 times the square root of the variance in sea surface elevation at frequencies 0.05–0.6 Hz [*Mei*, 1989]), or the ice draft when ice is present [*Magnell et al.*, 2010].

Wave hindcasts were made using the WAVEWATCH III® numerical wave model [*Tolman*, 2009], forced with the U.S. Navy's Fleet Numerical Meteorology and Oceanography Center (FNMOC) wind fields and ice products (derived from satellite passive microwave radiometers). Ice presence or absence was determined using a 25% threshold [*Tolman*, 2003].

Fetch estimates were made using the NSIDC [*National Snow and Ice Data Center*, 2012] 4 km daily ice product and calculating the distance along the direction of the FNMOC winds from the mooring location to an ice or land boundary. During the maximum open water period (September), the mooring is located such that the fetch distance exceeds 1000 km in all directions and the fetch calculation is a proxy for the basin scale.

Storm duration estimates were made as the cumulative hours during which FNMOC wind speed exceeded 5 m/s, with a reset to zero whenever the wind dropped below 5 m/s.

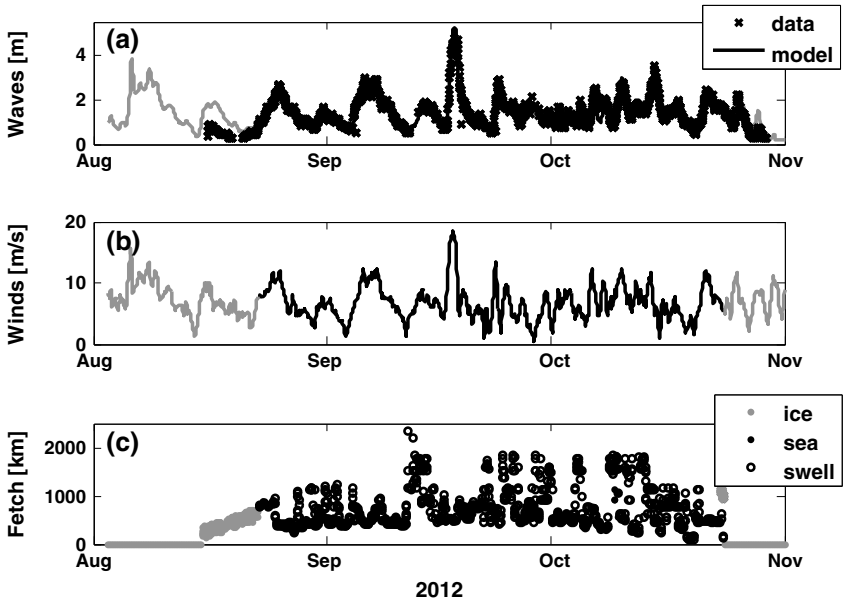

Figure 2. Time series of Arctic Ocean wave conditions. Hourly values for (a) significant wave height, (b) wind speed at 10 m reference height, and (c) fetch along the direction of the wind, from the mooring location to ice or land. In Figure 2a, symbols show the in situ observations, and the solid curve shows the model hindcast results. Gray is used to indicate the presence of partial ice cover (as determined from the mooring data). In Figure 2c, filled symbols are for wave conditions that are pure wind seas and open symbols are for wave conditions that include swells (as determined by nondimensional wave age, $\frac{c}{U}$).

3. Results

There is excellent agreement in wave height between the observations for most of the summer 2012 record and the model (Figure 2), but there is a notable bias in mid-August (i.e., immediately following the mooring deployment on 12 August) when the model overestimates the observations by as much as a factor of 2. This corresponds to the seasonal retreat and advance of sea ice, during which the NSIDC products indicate that partial cover occurs at the mooring location. The wave model includes methods for treating the effect of ice (using estimates of ice concentration as input), but it is believed that the ice products employed here, derived from satellite passive microwave radiometer, underrepresent the ice. Clearly, the local effects of ice on the waves at a given location are significant and warrant further investigation. Here, however, we focus on the regional effects of sea ice variations and examine the middle portion of the wave record, when the mooring location is ice free but ice cover farther north of the mooring location continues to control the effective size of the basin.

There were two notable wave events in 2012: a storm early August and another in mid-September. The first storm occurred before the in situ observations began (and when satellite observations suggest that ice cover was still significant at the mooring location); hence, only model results are shown for that storm. Although the first storm was significant in forcing ice retreat [*Parkinson and Comiso*, 2013], the waves associated with that storm were not modeled to be as large as the September storm. This is likely because the fetch available for wave growth was much smaller in August (when the ice edge was at approximately 72°N) than in September (when the ice edge was at approximately 80°N).

The overall dependence on open water distance is shown in Figure 3, where nondimensional wave energy scales with nondimensional distance over 3 orders of magnitude. (The points from the September storm, for example, lie near the regression line and span 10^4 to 10^6.) The coefficient of determination is $R^2 = 0.81$, which is significant beyond the 95% level and is notably higher than the direct correlation of wind speed and wave height ($R^2 = 0.67$, not shown). In contrast, there is no significant relation between nondimensional wave energy and nondimensional storm duration ($R^2 = 0.001$, not shown).

Scaling analysis such as this is often prone to spurious correlation, because the wind speed U is used in both variables. Here the lack of correlation between wave energy and duration, which also each have U in their

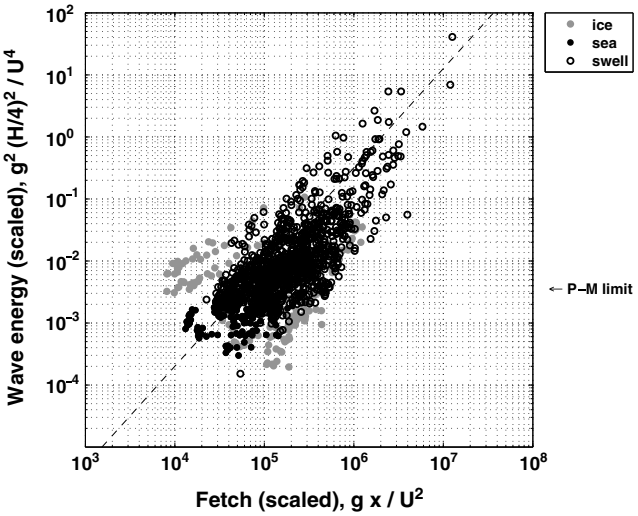

Figure 3. Scaling of waves in the Arctic Ocean, using nondimensional wave energy versus nondimensional fetch. There are 1880 points (each corresponding to an hourly observation from the in situ mooring at 75°N, 150°W). Symbols as in Figure 2. The dashed line is a regression with a logarithmic slope of 1.6. The Pierson–Moskowitz limit for pure wind seas is shown at $\mathcal{E} = 3.64 \times 10^{-3}$.

scaling, confirms that the fetch correlation is not spurious. Furthermore, there is no systematic dependence or correlation with wind direction, which is distributed nearly uniformly over the record in the range 0–15 m s^{-1}. Other relationships, however, are apparent in the data. Dimensionless peak period has a strong positive correlation with dimensionless fetch ($R^2 = 0.7$) and a dependence $\mathcal{X}^{1/2}$. Dimensionless energy has a strong correlation ($R^2 = 0.5$) with wave age and a dependence $(c/U)^4$.

The empirical scaling (Figure 3) obscures many of the details of the wave action balance and wave-ice interactions. In contrast to pure wind sea studies [*Dobson et al.*, 1989; *Stiassnie*, 2012], the scaling includes swell (e.g., dominant wave periods of up to 10 s during the September storm), and the values greatly exceed the Pierson–Moskowitz limit. The swell is not driven by the local wind and thus is an external source of wave energy in the scaling. To isolate points with swell, the points in Figure 3 are separated by nondimensional wave age, $\frac{c}{U}$, which is the ratio of the dominant wave celerity to the wind speed. Pure wind seas have a wave age less than one, indicating that the wind is driving the waves, and these points cluster largely below the Pierson–Moskowitz limit. Swells have a wave age greater than one, indicating that the waves are outrunning the wind, and these points extend well above the Pierson–Moskowitz limit. The seas have the expected dependence of $\mathcal{X}^1$, whereas the swells have a dependence closer to $\mathcal{X}^{1.7}$. The overall fit is $\mathcal{X}^{1.6}$.

The scaling is successful across both categories, because these waves represent a continuum of sea and swell. The synoptic wind fields that drive the wind sea are large enough in scale to be relevant to the whole basin as the wind sea evolves into swell. This is similar to the results of *Young* [2006], in which both sea and swell follow a fetch law in Hurricanes (his Figure 11) because under extreme forcing the swell remains part of the wind and wave system. Here the distance of open water is relevant to the nonlinear interactions that control the development of swells (because the nonlinearity is weak and requires large propagation distances) [*Hasselmann*, 1962]. In the limit of pure swell, the local wind is not important, but the scaling of wave height and basin size is still valid because space is required to build the swell. For swells, the length scale $\mathcal{X}$ can be interpreted as the basin scale (although the actual fetch is still used), because a mooring in the center of the basin will have a similar value (regardless of wind direction) that represents the characteristic distance to an ice boundary.

4. Conclusion

The Arctic Ocean is unique in annual variation of length scale, with the maxima increasing dramatically in recent years. Although the dynamics are more general than the conventional fetch dependence of ocean waves, the result is simple: open water distances are the controlling variable for wave heights in the Beaufort Sea (and likely the rest of the Arctic Ocean). Future scenarios for reduced seasonal sea ice cover in the Arctic suggest that larger waves are to be expected and that swells will be more common. Swells carry more energy and have longer attenuation scales within ice [*Squire et al.*, 1995; *Squire*, 2007] and thus will be more effective at breaking up the remaining ice. It is possible that the increased wave activity will be the feedback mechanism which drives the Arctic system toward an ice-free summer. This would be a remarkable departure from historical conditions in the Arctic, with potentially wide-ranging implications for the air-water-ice system and the humans attempting to operate there.

The increasing wave climate will also have implications for the coasts, which are already eroding rapidly during summer months as a result of climate change and subsequent loss of permafrost [*Overeem et al.*, 2011]. Using the conventional approach that shoreline sediment transport depends primarily on incident wave energy [*Bailard*, 1981], the expectation then is for coastal erosion to increase with a similar $\mathcal{X}^{1.6}$ dependence on the open water fetch of the Arctic Ocean. Although the actual wave effects will of course be site specific and complex, our scaling is a starting point in understanding the rapidly changing wave climate in the Arctic Ocean and the likely expanding future role of waves in the Arctic system.

Acknowledgments

We acknowledge the financial support of the Office of Naval Research and the logistical support of Rick Krishfield and the Beaufort Gyre Exploration Project (BGEP) team at the Woods Hole Oceanographic Institution.

The Editor thanks Alexander Babanin and an anonymous reviewer for their assistance in evaluating this paper.

References

Alves, J. H. G. M., M. L. Banner, and I. R. Young (2003), Revisiting the Pierson–Moskowitz asymptotic limits for fully developed wind waves, *J. Phys. Oceanogr.*, *33*(7), 1301–1323, doi:10.1175/1520-0485(2003)033<1301:RTPALF>2.0.CO;2.

Bailard, J. A. (1981), An energetics total load sediment transport model for a plane sloping beach, *J. Geophys. Res.*, *86*(C11), 10,938–10,954.

Battjes, J. (1988), Surf-zone dynamics, *Annu. Rev. Fluid Mech.*, *20*, 257–293.

Bogucki, D. J., W. M. Drennan, S. Woods, S. Gremes-Cordero, D. G. Long, and C. Mitchell (2013), Short surface waves in the Canadian Arctic in 2007 and 2008, *J. Geophys. Res. Oceans*, *118*, 3712–3722, doi:10.1002/jgrc.20273.

Dobson, F., W. Perrie, and B. Toulany (1989), On the deep-water fetch laws for wind-generated surface gravity waves, *Atmos. Ocean*, *27*, 210–236.

Dozaki, M., T. Hayakawa, and S. Sakai (1999), Field observation on wave-ice interactions in the Okhotsk Sea, in *Proceedings of the 9th International Offshore and Polar Engineering Conference*, vol. 2, edited by J. S. Chung, pp. 628–635, Int. Soc. of Offshore and Polar Eng., Cupertino, Calif.

Fontaine, E. (2012), A theoretical explanation of the fetch- and duration-limited laws, *J. Phys. Oceanogr.*, *43*(2), 233–247, doi:10.1175/JPO-D-11-0190.1.

Francis, O. P., G. G. Panteleev, and D. E. Atkinson (2011), Ocean wave conditions in the Chukchi Sea from satellite and in situ observations, *Geophys. Res. Lett.*, *38*, L24610, doi:10.1029/2011GL049839.

Hasselmann, K. (1962), On the non-linear energy transfer in a gravity-wave spectrum Part 1. General theory, *J. Fluid Mech.*, *12*, 481–500, doi:10.1017/S0022112062000373.

Hasselmann, K., et al. (1973), Measurements of wind-wave growth and swell decay during the Joint North Sea Wave Project (JONSWAP), *Erganzungsheft Dtsch. Hydrogr. Z. Reihe*, *A*(8), (Nr. 12), 95 pp.

Magnell, B., L. Ivanov, and E. Siegel (2010), Measurements of ice parameters in the Beaufort sea using the Nortek AWAC acoustic Doppler current profiler, in *Proceedings of the Oceans 2010 Conference*, MTS/IEEE, Seattle, Wash.

Marko, J. R. (2003), Observations and analyses of an intense waves-in-ice event in the Sea of Okhotsk, *J. Geophys. Res.*, *108*(C9), 3296, doi:10.1029/2001JC001214.

Mei, C. (1989), *The Applied Dynamics of Ocean Surface Waves, Advanced Series on Ocean Engineering*, vol. 1, World Sci., Singapore.

Melville, W. K. (1996), The role of surface-wave breaking in air-sea interaction, *Annu. Rev. Fluid Mech.*, *28*, 279–321.

National Snow and Ice Data Center (2012), IMS daily northern hemisphere snow and ice analysis at 4 km and 24 km resolution, http://nsidc.org/data/g02156, Natl. Snow and Ice Data Cent., Boulder, Colo. [Updated daily.]

Overeem, I., R. S. Anderson, C. W. Wobus, G. D. Clow, F. E. Urban, and N. Matell (2011), Sea ice loss enhances wave action at the Arctic coast, *Geophys. Res. Lett.*, *38*, L17503, doi:10.1029/2011GL048681.

Parkinson, C. L., and J. C. Comiso (2013), On the 2012 record low Arctic sea ice cover: Combined impact of preconditioning and an August storm, *Geophys. Res. Lett.*, *40*, 1356–1361, doi:10.1002/grl.50349.

Pierson, W. J., Jr., and L. Moskowitz (1964), A proposed spectral form for fully developed wind seas based on the similarity theory of S. A. Kitaigorodskii, *J. Geophys. Res.*, *69*, 5181–5190.

Schwendeman, M., J. Thomson, and J. Gemmrich (2014), Wave breaking dissipation in a fetch-limitted sea, *J. Phys. Oceanogr.*, *44*(1), 104–127.

Showstack, R. (2013), Diminishing sea ice in the Arctic presents challenges and opportunities, *Eos Trans. AGU*, *94*(31), 270–271, doi:10.1002/2013EO310002.

Simmonds, I., and K. Keay (2009), Extraordinary September Arctic sea ice reductions and their relationships with storm behavior over 1979–2008, *Geophys. Res. Lett.*, *36*, L19715, doi:10.1029/2009GL039810.

Squire, V. A. (2007), Of ocean waves and sea ice revisited, *Cold Reg. Sci. Technol.*, *49*, 110–133.

Squire, V. A., J. P. Dugan, P. Wadhams, P. J. Rottier, and A. K. Liu (1995), Of ocean waves and sea ice, *Annu. Rev. Fluid Mech.*, *27*, 115–168.

Squire, V. A., G. L. Vaughan, and L. G. Bennetts (2009), Ocean surface wave evolvement in the Arctic Basin, *Geophys. Res. Lett.*, *36*, L22502, doi:10.1029/2009GL040676.

Steele, M., J. H. Morison, and N. Untersteiner (1989), The partition of air-ice-ocean momentum exchange as a function of ice concentration, floe size, and draft, *J. Geophys. Res.*, *94*, 12,739–12,750.

Stephenson, S. R., L. C. Smit, and J. A. Agnew (2011), Divergent long-term trajectories of human access to the Arctic, *Nat. Clim. Change*, *1*, 156–160.

Stiassnie, M. (2012), Fetch-limited growth of wind waves, *J. Geophys. Res.*, *117*, C00J04, doi:10.1029/2011JC007579.

Stroeve, J., M. Serreze, S. Drobot, S. Gearheard, M. Holland, J. Maslanik, W. Meier, and T. Scambos (2008), Arctic sea ice extent plummets in 2007, *Eos Trans. AGU*, *89*, 13–14.

Stroeve, J. C., M. C. Serreze, F. Fetterer, T. Arbetter, W. Meier, J. Maslanik, and K. Knowles (2005), Tracking the Arctic's shrinking ice cover: Another extreme September minimum in 2004, *Geophys. Res. Lett.*, *32*, L04501, doi:10.1029/2004GL021810.

Tolman, H. L. (2003), Treatment of unresolved islands and ice in wind wave models, *Ocean Model.*, *5*, 219–231.

Tolman, H. L. (2009), User manual and system documentation of WAVEWATCH III version 3.14, *Tech. Rep. 276*, NOAA/NWS/NCEP/Marine Modeling and Analysis Branch, Camp Springs, Md.

Young, I. (1999), *Wind Generated Ocean Waves*, Elsevier Ocean Engineering Book Series, Elsevier, New York.

Young, I. R. (2006), Directional spectra of hurricane wind waves, *J. Geophys. Res.*, *111*, C08020, doi:10.1029/2006JC003540.